DISTRIBUTION OF CURRENT CONVERSION IN POROUS GAS ELECTRODES

Karl Joachim Euler

VARTA
Frankfurt/Main, Germany

§ 1 Introduction, Problems

During the past years, the phenomena of current conversion in porous gas electrodes of finite thickness have been investigated very thoroughly by a great number of authors (2, 3, 4, 5, 6, 7, 8, 9). The main attention in recent papers was paid to the investigation of the current conversion in the nearest neighbourhood of thriphase zones, i.e. nearest to the liquid - gas meniscus in a single pore of the working electrode, see below § 5. However, this is only one of several important factors, responsible for the distribution of current conversion inside electrodes of finite thickness. In the following paper, plaine porous gas electrodes consisting of at least two layers, having different pore diameters, are examined. To this kind of electrodes, the gas is fed through one surface, and the liquid electrolyte adheres the other electrode surface. Thickness is supposed to be finite but small with regard to the lateral dimensions, and the use of electrolyte repellent agents may be generally excluded*).

§ 2 General Theory

In most cases, the complicated theory of tri-phase electrodes can be reduced to the better known (9, 12)

*) Please see § 7

theory of porous two-phase electrodes. Figure 1 shows the geometry of a semi-infinite porous double layer oxygen electrode, made of metal powder. The electronic conductivity of the electrode matrix is supposed to be high, to such a degree, that the voltage drop in the electron path can be neglected. In the cover layer, the narrow pores are filled completely with electrolyte, and no electrical conversion of ions to electrons proceeds therein. Thus, the cover layer acts as simple resistor in the electric analogue, having no influence on the spatial distribution of current conversion inside the working layer.

When we regard, for instance, a hydrogen anode in alkaline electrolyte, the electrochemical gross reaction may be written

$$H_2 + 2\ OH^- \longrightarrow 2\ H_2O + 2\ e^-.$$

Since "metabolism waste" water is formed, which must be removed from the working layer, either migrating in the liquid phase, or diffusing, as steam, into the hydrogen supply system. Because the water lowers the ionic conductivity inside the electrode, its effect approximatively can be taken into consideration, under steady state conditions, by introduction of a somewhat elevated ionic resistivity $\bar{\rho}_i$, see § 8.

§ 3 Special Transport Function θ

Consequently, only two transport phenomena remain to be considered, the ion resistivity, and the gas friction inside the narrow pores, hereafter called "gas resistivity". Two-phase electrodes, up to now have been treated as an electrical network. Mechanical characteristics, like diffusion constant D of gases, pressure drop, and channel geometry must be transferred into adequate electrical magnitudes.

Using the Einstein equation $D = b\ kT/e$, immediately a gas resistivity ϱ_g can be defined:

$$1/\varrho_g = nN\ b\ e = D\ nN\ e^2/kTf,$$

$N\ [cm^{-3}]$	carrier density	$D\ [cm^2/s]$	diffusion constant
n	number of elementary charges per carrier	$kT/e \approx 25$ mV	at room temperature
		$f \approx 4$	geometrical factor, including porosity, tortuosity, etc.
$b\ [cm^2/Vs]$	"physical" mobility		
$e = 1{,}601 \cdot 10^{-19}$ As			

To be exact, the Einstein equation applies only to conductors having equal mobilities b_+ and b_- of carriers of both signs. Here, H^+ and OH^- ions are involved, the mobilities of which differ considerably. However, only an estimate is necessary in the framework of this investigation, as become evident here below.

Inserting figures as follows:

$0{,}1 < D < 1 \quad cm^2/s$ valid for gases at room temperature under nearly atmospheric pressure

$N \approx 5{,}3 \cdot 10^{19} \quad cm^{-3}$ $\begin{cases} \text{room temperature} \\ \text{pressure } 2\ kp/cm^2 \end{cases}$

$n = 1$; $e = 1{,}601 \cdot 10^{-19}$ As ; $f \approx 4$;

$kT/e = 25{,}3$ mV

we get $0{,}01 < \varrho_g < 0{,}1$ ohm·cm.

On the other hand, the ionic resistivity inside the working layer can be estimated easily, and, in addition, has been measured by Holthusen (11). Porosity is around 50 pct., and about 15 pct. thereof are filled with electrolyte, 6 n KCH at 60 °C. Taking into consideration a tortuosity factor of 1,5 , the final ionic resistivity can be calculated to $\varrho_i \approx 20$ ohm·cm. This result agrees well with Holthusens measurements.

When comparing gas and ionic resistivities, we find, that $\varrho_g \ll \varrho_i$. Thus, beneath electronic resistivity ϱ_e, also ϱ_g can be neglected.

Out of the theory of two-phase electrodes, we take

$$\theta(z^*) = \frac{a \cosh[\alpha S z^*] + c \cosh[\alpha S(1-z^*)]}{(a+c) \sinh[\alpha S]} \alpha S. \qquad \text{(eq.1)}$$

$a = \varrho_i/A$; $c = \varrho_g/A$; $\alpha^2 = (\varrho_i+\varrho_g)g$; $g = i/\psi$;

A [cm^2] area; ψ [mV] border overvoltage; i [mA/cm^2] current density.

Since equation 1 implies diffusion constant D and ion mobility b, we call Θ the "Special Transport Function" of this type of porous gas electrode. Because $\varrho_i > \varrho_g$ or $a > c$, the above written equation 1 can be simplified

$$\Theta_i(z^*) = \frac{\cosh\left[\sqrt{\varrho_i g}\, S\, z\right]^*}{\sinh\left[\sqrt{\varrho_i g}\, S\right]} \sqrt{\varrho_i g}\, S, \qquad \text{(eq. 2a)}$$

or, introducing $C = \sqrt{\varrho_i g}\, S$

$$\Theta_i(z^*) = \frac{C}{\sinh C} \cosh\left[C\, z^*\right], \qquad \text{(eq. 2b)}$$

the shape of this function being given in figure 2. $\Theta_i(z^*)$ is analogous to $\Theta(z^*)$ the <u>approximative</u> special transport function, neglecting gas resistance.

To let $\Theta(z^*)$ or $\Theta_i(z^*)$ become effective and evaluable, we have to introduce adequate values of boundary overvoltage ψ, or overvoltage parameter g, respectively. Under steady state conditions, i.e. a constant current density i flowing to or from the electrode, there may exist a factor of 10 or 100 between gas concentration (or activity) in the gas phase and electrolyte. Thus,

we are led to the conclusion, that a small "diffusion" potential ψ will occur across the boundary, similar to phenomena often observed on semiconductors. Using as approximation simply the Nernst equation $\psi = \frac{kT}{ze} \ln f_2/f_1$, wherein f_2 and f_1 devote the hydrogen activity within electrolyte and gas phase, respectively, we have to expect 15 to 60 mV in oxygen electrodes *), and 60 to 120 mV in hydrogen electrodes, respectively. Inserting current density i between 10 and 100 mA/cm^2, the range of possible values, in which $g = i/\psi$ must be comprised, is $0{,}1 < g < 10$. Figure 2 exhibits a set of special transport function, equation 2b, using as parameters $\rho_i = 20$ ohm·cm, $0{,}1 < g < 10$, and electrode thickness S = 1 mm.

§ 4 Statistical Distribution of Active Sites

With the special transport function $\Theta(z^*)$, the porous electrode has been described as homogeneous and isotropic continuum. The active sites, or, in other words, working grains of incorporated catalyst are supposed to be evenly distributed, and its activity shall not depend on z*. From observations made at a great number of electrodes, we know, that there exists a certain statistic distribution $Y(z^*)$ of active sites, depending on grain density statistics, grain size statistics, spatial distribution of active procedure, flooding of pores and on poisoning after a prolonged period of work. However, in general $Y(z^*)$ may

*) depending on electrode mechanism, i.e. reversible oxygen electrode, or formation of H_2

be regarded as even, $Y_o(z^*) \approx 1$. This approximation holds fairly well during the first year of use under rated load. Later on, expressions like $Y_t(z^*) \approx 1 - (mz^*)^q$, therein m depending on time, $0 < m < 1$, and $q > 1$, fit better. To avoid unadequate mathematical difficulties, we limit the study here to the behaviour of electrodes having active sites evenly distributed, $Y(z^*) = Y_o(z^*) \approx 1$.

§ 5 Current Distribution in a Single Pore

More than 100 years ago, already Sir Grove (1), had some insight into the import role of the tri-phase boundary as current generating zone of gas electodes. However, not earlier than during the past years, several authors tried to solve the problem of current conversion spatial distribution in these tri-phase zones, see for instance (3,4,5 and 6). The resulting distribution functions Φ (v) are with respect to a co-ordinate v along the single pore, or perpendicular to a single conversion zone.*) The origin v has to be imagined in the top of the meniscus, or simply centered to each individual conversion zone. z^* (or z) and v include an angle ψ depending on the geometrical situation of each site, see figure 3.

*) This treatment is not restricted to "pore" geometry, but can be easily applied to every geometry, just inserting as d the characteristic distance.

The distribution Φ (v) depends considerably on geometrical and physical assumptions, e.g. pore or film geometry, gas diffusion across liquid or solid phase, surface migration of gas atoms, creeping of electrolyte, electrochemical reaction, rate determining step, nature of wastes formed etc. However, as global characteristics, the simple rule can be regarded as generally valid in nearly all cases, that Φ (v) differs from zero only in a small interval $\pm \Delta v$ on both sides of the co-ordinate origin, and Δv being comparable to the characteristic "pore diameter" d. Consequently, each individual conversion site can approximately be treated as a small differential volume, perhaps as small cube or sphere, the diameter s of which is a little bit larger than the pore diameter d. In our special case, d is of the order of magnitude of 30 μm, and therefore small when compared with electrode thickness S.

§ 6 Combination of Θ, Y and Φ

Combining the aforementioned distributions, we get for <u>one</u> single conversion site

$$dJ/J = \Theta(z^*)\ Y(z^*)\ \Phi\ (v)\ \ dv. \qquad \text{(eq.3)}$$

Therein, Φ (v) is the distribution inside a single site, $Y(z^*)$ represents the probability, that sites are

located in a certain depth interval from z^* to z^*+dz^*, and $\Theta(z^*)$ indicates the fraction dJ of the overall current J converted in the zone z^* to z^*+dz^*. Since the problem, in fact, is to indicate the conversion profile inside the whole working layer , we have to integrate equation 3, taking into consideration the angle φ between the co-ordinates v and z^*. However, we restricted ourselves to $Y = Y_o(z^*) \approx 1$ and to such electrodes, whose thickness $S > d$ allows to approximate the individual sites as small point-like spheres. Then the influence of Φ and φ degenerates simply to a factor, which furthermore can be taken into account by normalizing the distribution with respect to the current J of the entire electrode. Thus, we get finally the spatial distribution of current conversion in the working layer of a semi-infinite, porous gas diffusion electrode

$$dJ(z^*)/J = \Theta_i(z^*)\, dz^* = \frac{C}{\sinh C} \cosh\left[C\, z^*\right] dz^*; \quad \text{(eq.4)}$$

Expression 4 do not depend on electrode area A, therefore dJ/J can be taken, at will, as current, or current density. In most practical cases, the columetric current load of the eletrode will be the favourized, because mostly obvious magnitude

$$\frac{di(z^*)}{i\, dz^*} = \frac{dJ(z^*)}{J\, dz^*} = \frac{C}{\sinh C} \cosh\left[C\, z^*\right]. \quad \text{(eq.5)}$$

to be measured in mA/cm^3.

§ 7 Penetration Depth

Since the current conversion in the electrodes under consideration is described by monotonous functions without maxima or minima, it may be useful, to define a penetration depth in the absolute z-scale

$$\cosh\left[\sqrt{\varrho_i g}(S-\tau)\right] = \frac{1}{e}\cosh\left[S\sqrt{\varrho_i g}\right],$$

e: basis of natural logarithms.

As easily event, this expression loses its sense, if $\cosh C < e$. Therefore, we let rise the electrode thickness S to very high values, than we are able to replace $\cosh\left[z \gg 1\right] \approx \frac{1}{2}\exp z$, and we get $\tau \approx -1/\sqrt{\varrho_i g}$. Table 1 contains calculated penetration depths in the ranges of g and ϱ_i here of interest.

Table 1 Penetration depth τ of conversion current in the working layer of a semi-infinite porous gas diffusion electrode, as function of boundary overvoltage parameter g and ionic resistivity ϱ_i.

g ($ohm^{-1}\ cm^{-3}$)	specific ion resistivity ρ_i (ohm·cm) 20	30	40	50	60	80
	penetration depth τ (mm)					
o,1	7,o2	5,73	4,95	4,45	4,o4	3,51
o,2	5,oo	4,o8	3,53	3,17	2,89	2,50
o,5	3,15	2,57	2,22	2,oo	1,82	1,58
1	2,25	1,84	1,59	1,42	1,30	1,13
2	1,58	1,29	1,12	1,oo	o,91	o,79
5	1,oo	o,82	o,71	o,63	o,58	o,5o
1o	o,7o	o,57	o,5o	o,44	o,4o	o,35
2o	o,5o	o,41	o,35	o,32	o,29	o,25

In the working layer of manufactured sintered nickel electrodes penetration depth has been found between o,6 and o,9 mm. These results refer to electrodes of different design, both oxygen cathodes and hydrogen anodes, containing fine divided silver metal, and Raney nickel as catalysts, respectively. Having in mind, that under steady load the mean ion resistivity $\bar{\rho}_i$ appears somewhat elevated above 20 ohm·cm*), the measured penetration depths agree fairly well with the results given in table 1. Consequently, the experimental range of g, has to be assumed to about $5 < g < 10$, i.e. the upper limit of the

*) see § 9.

range indicated in § 3. The reason probably for it, is, that the border overvoltage ψ really is somewhat lower, than evaluated from the normal Nernst equation. However, already Nernst (12) pointed out clearly, that "diffusion" potentials can be much lower, depending on the mobility quotient and on the sign of the second term within the brakes in a straight forward equation indicated also by Nernst:

$$\psi = - \frac{kT}{ne} \frac{b_+ - b_-}{b_+ + b_-} \left[\ln \frac{f_2}{f_1} + B(\sqrt{f_2} - \sqrt{f_1}) \right]. \qquad \text{(eq.5)}$$

wherein b_+ and b_- are the moblities of positive and negative ions, f_1 and f_2 are hydrogen activities in the gas phase and the electrolyte, and B is a constant, the magnitude and sign of which depend on the mutual interaction of ion strength, activity factors, and electrophoresis. Assuming $b_+ = 33 \cdot 10^{-4}$ and $b_- = 18 \cdot 10^{-4}$ cm^2/Vs, the mobility quotient equals $\approx$ o,3 . When we approximate $B \approx 0$, then we finally find numerical values of ε up to 30 $ohm^{-1} cm^{-3}$.

§ 8 Carbon Electrodes

Instead of multiple hydrophilic layers having different porse size, gas phase and electrolyte can be throughout separated by impregnating uniform porous electrodes with electrolyte repellent agents. This is effected, preferably on carbon electrodes, by adding solid hydrocarbons, nitrobenzene, synthetic rubber, silicones, polyethylene (PE)

or even polytetrafluoro-ethylene (PTFE). Schumacher and Heise (13) showed already, that "hydrophobic" monolayer electrodes can be manufactured only either not completely electrolyte repellent but correctly working, or, on the other side, completely hydrophobic but not properly suited to their electrochemical duties.

During the past years, very thin triple layer carbon electrodes have been developed by Kordesch (14). These electrodes consist of a sintered nickel foil as substrate, about o,18 mm in thickness, and completely water repellent by addition of some PTFE. On this supporting sheet, a coarse carbon layer is sprayed, composed of 50 pct of carbon powder and 50 pct PTFE and PE. This inner, so-called "backing" carbon layer incorportes no catalyst. Its thickness is about o,25 mm. Finally, the electrode is covered by a third layer, consisting of 75 pct of carbon and 25 pct ~~PTE~~ PTFE, having also about 2 mg/cm^2 of platinum black as catalyst. The thickness of this upper, so-called "active" carbon layer is about o,13 mm.

The large amounts of electrolyte repellent agents incorporated in the two under layers, holds them free of electrolyte.. However, in the upper layer, the PTFE acts preferably as binding agent and, therefore, this active layer is partly filled with electrolyte. This kind of

electrodes are designed for a very low gas pressure, less than o,1 kp/cm^2 gage. Therefore, already the very thin film of electrolyte, adherent to the outer surface of the electrode avoid gas losses.

In principle, multilayer, partly hydrophobic electrodes obey the same theory as hydrophilic two-layer arrangements. Only a thorough study of the parameters is required in those cases.

Since the active layer exhibit a thickness of no more than o.13 mm, we are led to the conclusion, that, in hydrophobic carbon electrodes ϱ_i and/or g must be higher, than in hydrophilic nickel sintered electrodes. In fact, both assumptions are reasonable. Electrolyte films on a partly repellent substraten often will be interrupted. Therefore, the main ion resitivity of the electrolyte network becomes substantially higher, than on hydrophilic materials. In carbon electrodes, the reaction gases are fed to the converting sites through very narrow slits and channels in the solid material rather than dissusion across liquid films. Thus, the activity between gas phase and electrolyte, in this type of electrode differs certainly less, than in hydrophilic ones. Consequently, the overvoltage ψ , as caused by this difference must be lower, $g \sim 1/\psi$ must be higher.

Thus, it seems likely, that gas restivity ϱ_g and electron resistivity ϱ_e remain small as compared to ion resistivity ϱ_i , $\varrho_e \ll \varrho_i$ and $\varrho_g \ll \varrho_i$. Since exact values of porosity, pore diameter, and fraction of pores filled have not been published, a quantitative comparison with the theory cannot yet be accomplished.

§ 9 Non-uniform Ion Resistivity

In a recent paper (15), it has been shown, that "strange"*) types of current distributions occur in porous electrodes, if ion and electron resistivities do not remain homogeneous, but depend on thickness co-ordinate z^*. Under steady state conditions, in hydrogen anodes water is formed, and in oxygen cathodes water is consumed. Thus, concentration profiles $K(z^*)$ occur, which influences ion conductivity. The "zero current" electrolyte exhibit nearly the ion resistivity minimum, and any change in concentration K will, therefore, cause an increase of ion resistance ρ_i. However, the exact concentration -and therefore also resistivity- profile is so far not yet known.

However, the influence of resistance profiles $\rho_i(z^*)$ can be studied without exact knowledge of their magnitude, simply by putting different oblique profiles into the electrical analogues. As a first series, we took <u>linear</u> concentration profiles $K(z^*)$:

$$K(z^*) = K_1 - K_2(1-z^*) \quad , \; z^* = z/S \qquad \text{(equ. 6a)}$$

having different constants K_2. In figure 4, the influence of three linear concentration profiles on current distribution is given.

*) i.e. distributions exhibiting a maximum inside the electrode, instead of a broad minimum as in "common" distributions

Table 2

Concentration profile parameters in figure 4

curve No in fig.4	type of profile	KOH concentration $K(z^*)$ in pct. of weight at $z^* = 0$	at $z^* = 1$
(1)	const.	27	27
(2)	linear	13,5	27
(3)	linear	4,5	27
(4)	linear	o,27	27

In general the influence even of very steep concentration profiles is not very important. Therefore, figure 4 to 6 are given in a logarithmic scale. Indicated is the relative fraction of current converted in a thin sheet Δz = o,1 mm of the electrode, given in pct. of the entire electrode current. As become evident, the concentration profile lowers the current distribution near the gas side of the electrode, i.e. near $z \approx 0$. In other words, the penetration depth has been decreased.

In order to verify this result, as a second series, we also took some other ion resistivity profiles into the analogue. The result indicated in figure 5 does not differ considerably from the influence of linear concentration profiles, as is evident when comparing fig. 4 and 5.

Table 3

Concentration profiles of figure 5

curve No in fig.5	type of profile	KOH concentration $K(z^*)$ in pct.of weight at $z^* = 0$	at $z^* = 1$
(1)	const.	27	27
(2)	linear	4,5	27
(3)	exp.	4,5	27
(4)	tgh	o,5	26

Exponential and tgh profiles are given by

$$K(z^*) = K_1 \quad \exp\left[-K_2(1-z^*)\right] \qquad \text{(equ. 6 b)}$$

and

$$K(z^*) = \frac{K_1}{2} + K_3 \quad \text{tgh}\left[K_4\left(\frac{1}{2} - z^*\right)\right]. \qquad \text{(equ. 6 c)}$$

As main result, we can state, that concentration profiles in the electrolyte do not cause unusual distributions of the current conversion in porous triphase electrodes. Especially, "strange" distributions do <u>not</u> occur here.

§ 10 Non-uniform Overvoltage

In order to replenish the results, in figure 6 the influence of overvoltage profiles on current distribution in porous triphase electrodes is shown, either having

uniform ion resistivity (curve 2), either in combination with exponential concentration profiles (curve 3). Already in (14) it was explained, that overvoltage profiles influences the distribution of current conversion much less, than resistivity profiles do. The profile chosen here is very steep; a nine-fold increase of overvoltage over a distance of only 1 mm, is completely out of the range to be ever expected in manufactured electrodes. Therefore, it can be affirmed, that also in porous triphase electrodes, the influence of realistic overvoltage profiles remains small. Even taking steep overvoltage profiles into consideration, no uncommon distributions occur in those triphase electrodes under consideration.

Table 4

Concentration and overvoltage profiles in figure

curve No in fig.6	KOH concentration $K(z^*)$ (pct. of weight)			overvoltage (z^*) (relative units)		
	type of profile	at $z^* = 0$	at $z^* = 1$	type of profile	at $z^* = 0$	at $z^* = 1$
(1)	const.	27	27	const.	1	1
(2)	const.	27	27	linear	9	1
(3)	exp.	4,5*)	27	linear	9	1

*) the same concentration profile as curve (3) in figure 5

Conclusion

The treatment of current conversion and its distribution inside the working layer of porous gas electrodes -tri-phase electrodes- can be substantially simplified by reducing the problem to the much better known theory of porous electrodes. The only condition ist, that electron resistivity can be neglected, as it is the case for instance in all practical fuel cell electrodes. To realize this theory, gas supply can be characterized by a "gas resistivity" to be measured in electrical units.

The distribution of current conversion can be found out as the product of three main factors, the special transport function Θ, the current distribution in a single current generating site, and the site statistics. The first of these factors governs the conversion behaviour at least of sintered metal electrodes. As a principal result of the work reported here, following the rules mentioned above, monotonous distribution curves can be given. A penetration depth can be defined, having the order of several tenth of a millimeter. The results agree with practical experience. By introducing concentration and/or overvoltage profiles, the theory can be further developed. As special result, no "strange" distributions occur under these conditions.

References :

1. R. G r o v e : On a Gaseous Voltaic Battery, Phil. Mag. 21 (1842) pp. 417 - 420

2. L. G. A u s t i n : Fuel Cells, NASA S P - 120, Washington, D. C., pp. 303 - 321, 1967

3. A. B o r u c k a and J. N. A g a r : An Electric Analogue for Meniscus Gas Electrodes, Electrochimica Acta 11 (1966) pp. 603-624

4. E. J u s t i and A. W i n s e l : Kalte Verbrennung - Fuel Cells, Franz-Steiner-Verlag, Wiesbaden, 1962, pp. 88 - 94

5. A. W i n s e l : Statistisches Modell einer Gasdiffusionselektrode, Advanced Energy Conversion 3 (1963) pp. 677 - 708 and 5 (1965) pp. 173-181

6. F. G. Will : Electrochemical Oxydation of Hydrogen on Partially Immersed Platinum Electrodes, Journ. Electrochem. Soc. 110 (1963) pp. 145 - 151

7. M. Bo n n e m a y, C. B e r n a r d, G. B r o n o ë l, D. D o n i a t, E. L e v a r t, G. P e s l e r b e et A. A. P i l l a : Etude expérimentale des électrodes poreuses. Les piles à combustible, ouvrage collectif, Paris 1965, p. 103 à 125

8. R. B u v e t : Origine des phénomènes de polarisation dans les électrodes poreuses. Les piles à combustible, ouvrage collectif, Paris 1965, p. 27 à 46

9. I. Gurevich and V. S. Bagotskij: Porous-Electrode Polarization, Electrochimica Acta 12 (1967) pp. 593 - 614

10. H. Holthusen: Untersuchungen über Knallgaszellen in Eloflux-Anordnung, Diploma Thesis, Technical University Braunschweig, Fed. Rep. Germany, Dec. 15, 1966, to be published soon

11. see for instance J. Euler and W. Nonnenmacher: Stromverteilung in porösen Elektroden, Electrochimica Acta 2 (1960) pp. 268 - 286

12. W. Nernst: Über die elektromotorische Wirkung der Ionen, Z. f. physikalische Chemie 4 (1889) pp. 129 - 181

13. E. A. Schumacher and G. H. Heise: The Alkaline Cell with Copper Oxide or Air Depolarization, Journ. Electrochem. Soc. 99 (1952) pp. 191 C - 196 C

14. K. Kordesch: Thin Carbon Electrodes, Proc. 21st Annual Power Sources Conference, Fort Monmouth 1967, pp. 14 - 16

15. K. J. Euler: Anomale Verteilung der Stromkonversion im Inneren poröser Zweiphasenelektroden, Electrochimica Acta, under press

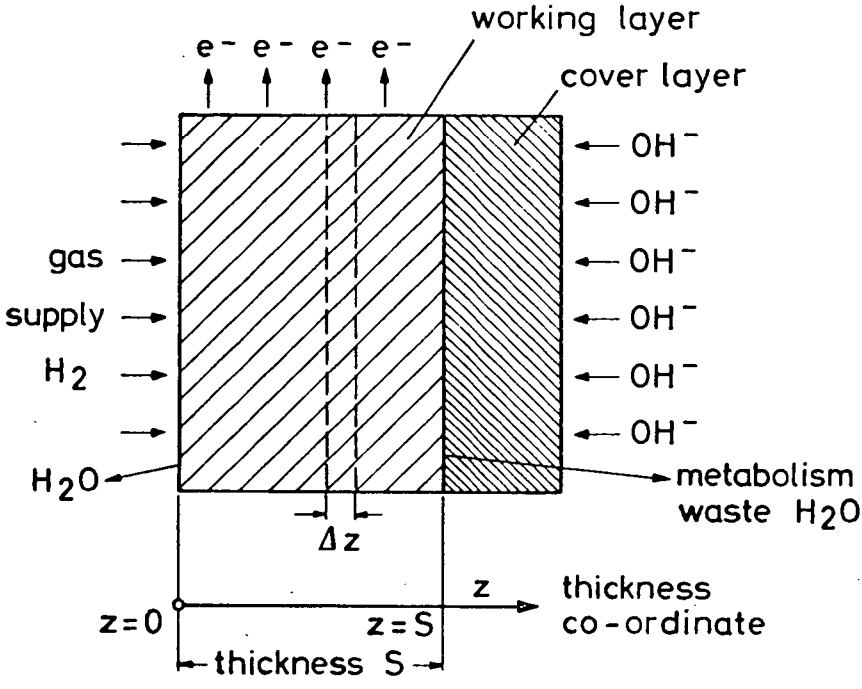

Figure 1

Geometry of the semi- infinite porous double layer electrode investigated here.

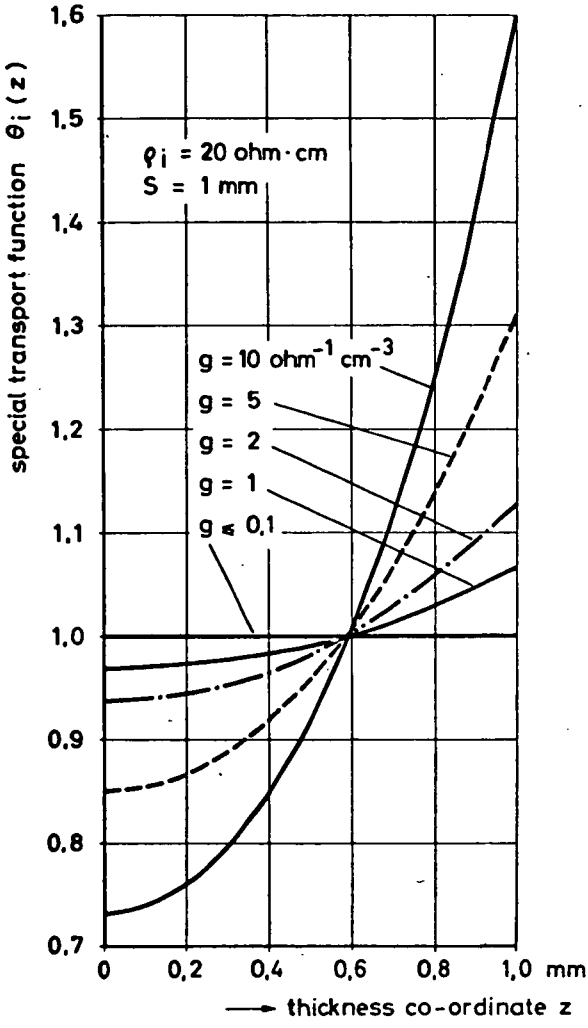

Figure 2

Shape of special transport functions $\Theta_i(z^*)$ in working layers of porous gas electrodes, equation 2 a or 2 b.

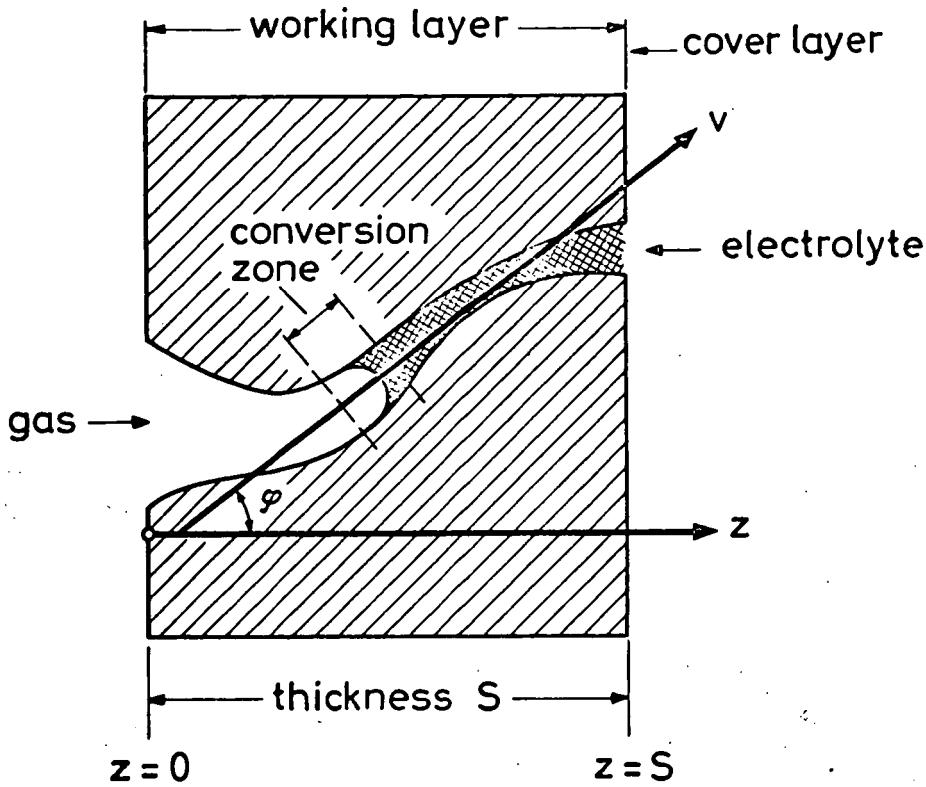

Figure 3

Relations between electrode co-ordinate z and individual site co-ordinate v. $z^* = z/S$.

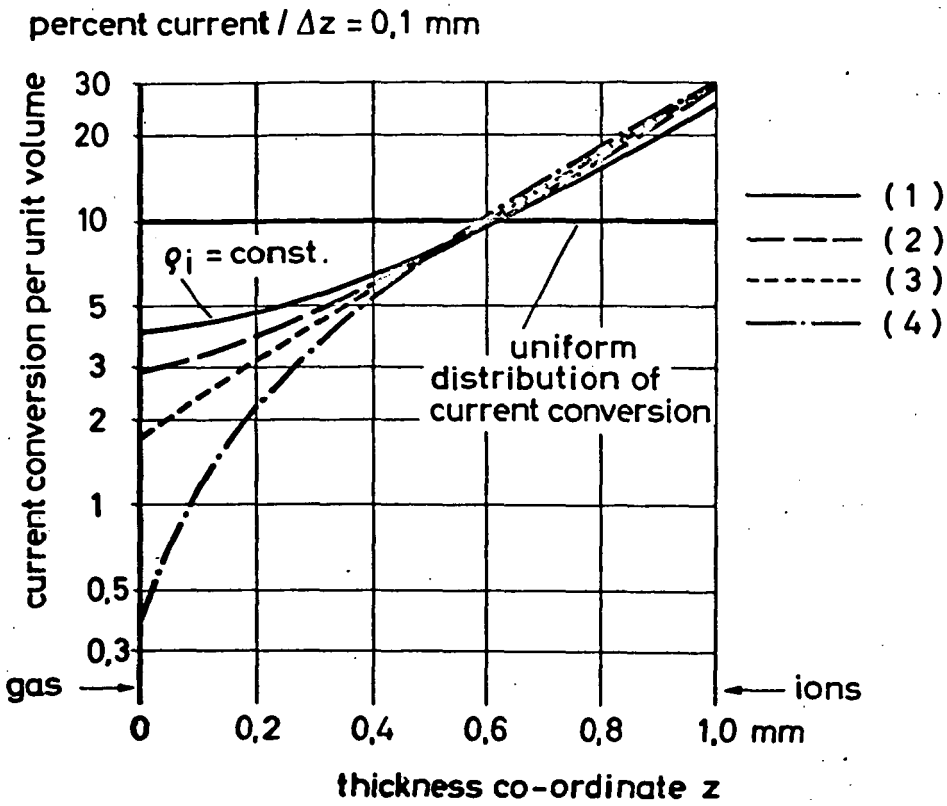

Figure 4

Influence of linear concentration profiles K(z) on current distribution in porous triphase electrodes. Thickness of working layer S = 1 mm, overvoltage parameter g = 10 $ohm^{-1}cm^{-3}$. Concentration profile parameters are given in table 2.

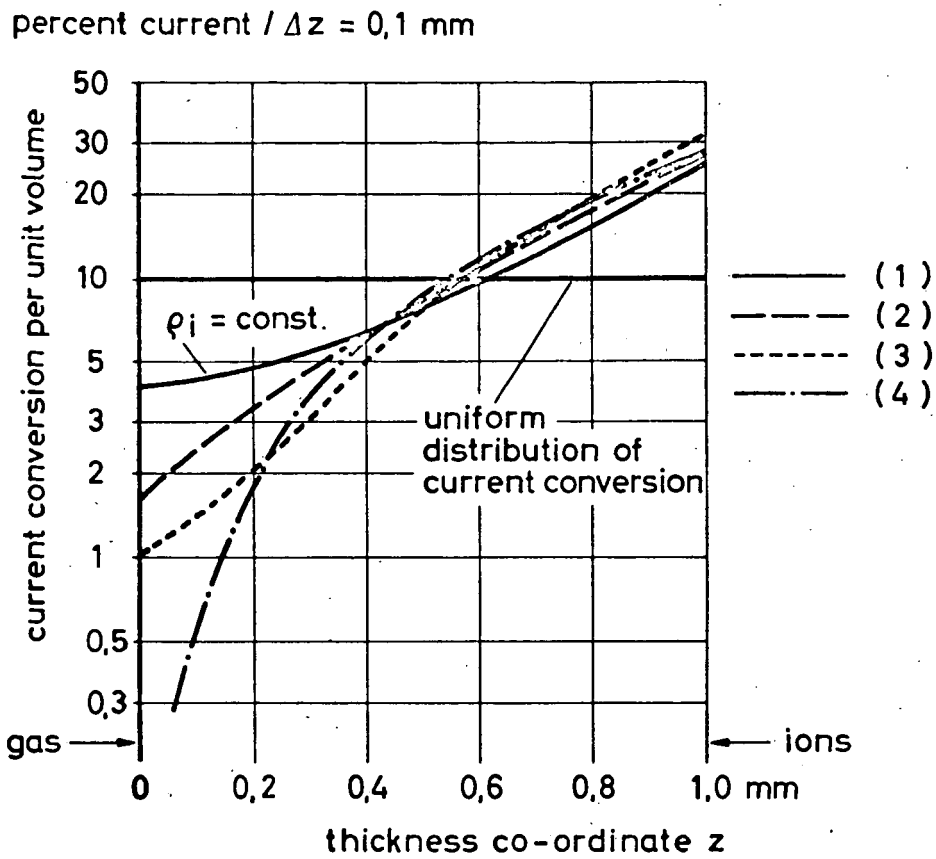

Figure 5

Influence of different shape of the concentration profile K(z) on current distribution in porous triphase electrodes. Thickness of working layer S = 1 mm, overvoltage parameter g = 10 $ohm^{-1}cm^{-3}$. Concentration profiles are given in table 3.

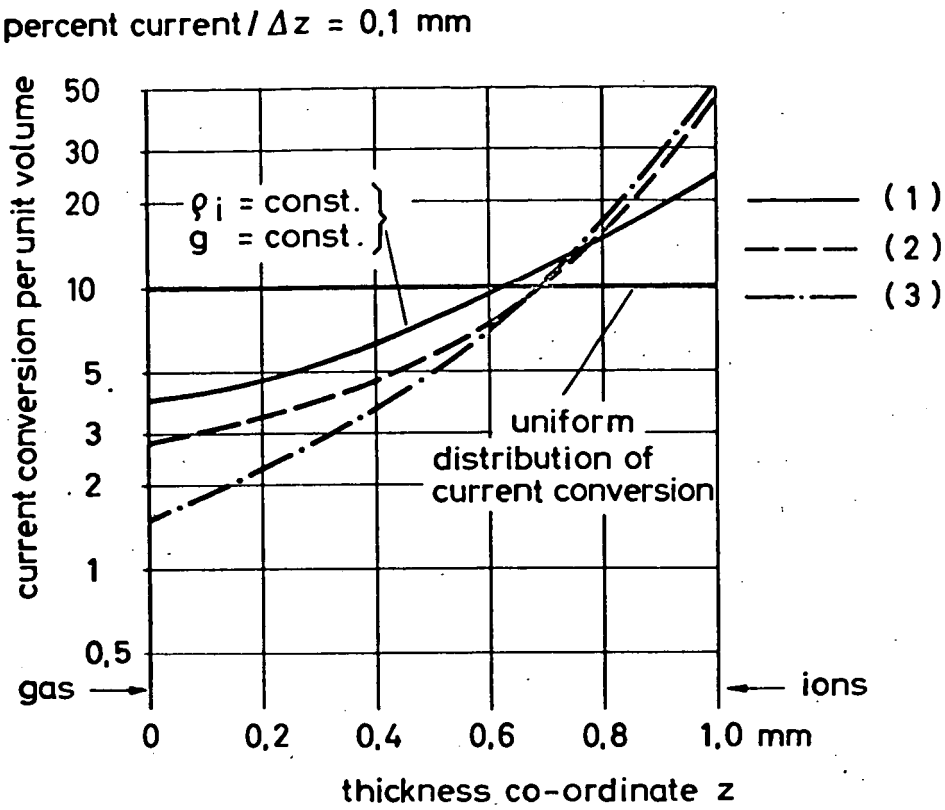

Figure 6

Influence of a linear overvoltage profile $\psi(z)$ on current distribution in porous triphase electrodes. Thickness of working layer S = 1 mm, parameters indicated in table 4.